

Theory of light emission from quantum noise in plasmonic contacts: above-threshold emission from higher-order electron-plasmon scattering

Kristen Kaasbjerg^{1,2,*} and Abraham Nitzan²

¹*Department of Condensed Matter Physics, Weizmann Institute of Science, Rehovot 76100, Israel*

²*School of Chemistry, The Sackler Faculty of Exact Sciences, Tel Aviv University, Tel Aviv 69978, Israel*

(Dated: December 7, 2024)

We develop a theoretical framework for the description of light emission from plasmonic contacts based on the nonequilibrium Green function formalism. Our theory establishes a fundamental link between the finite-frequency quantum noise and AC conductance of the contact and the light emission. Calculating the quantum noise to higher orders in the electron-plasmon interaction, we identify a plasmon-induced electron-electron interaction as the source of experimentally observed above-threshold light emission from biased STM contacts. Our findings provide important insight into the effect of interactions on the light emission from atomic-scale contacts.

PACS numbers: 73.63.-b, 72.70.+m, 73.20.Mf, 68.37.Ef

Atomic-size contacts [1], realized, e.g., in scanning tunneling microscopy (STM), provide a unique platform to study fundamental quantum transport phenomena such as, e.g., conductance quantization [2], suppression of shot noise [3], and vibrational inelastic effects on the conductance and shot noise [4, 5]. Recently, light emitted from STM contacts due to inelastic electron scattering off localized plasmons was used as a probe of the shot noise at optical frequencies [6]. Apart from standard emission due to one-electron scattering processes with photon energy $\hbar\omega < eV$, the observation of above-threshold emission with $\hbar\omega > eV$ indicates that interaction effects on the noise are probed [6, 7]. Emission from atomic-scale contacts is thus well-suited for studying the fundamental properties of high-frequency quantum noise.

The role of quantum noise as excitation source of electromagnetic fields is known from theoretical work on mesoscopic conductors [8–11]. The emission is related to the positive frequency part, $\mathcal{S}(\omega > 0)$, of the *asymmetric* quantum noise

$$\mathcal{S}(\omega) = \int dt e^{-i\omega t} \langle \delta I(0) \delta I(t) \rangle, \quad (1)$$

where $\delta I = I - \langle I \rangle$ and I is the current operator, whereas the absorption is connected to the negative frequency part, $\mathcal{S}(\omega < 0)$. The study of finite-frequency noise and the associated emission has been attracting attention in atomic-scale [6, 7], molecular [12–16] and mesoscopic conductors [17–27], and may shed light on fundamental issues in molecular optoelectronics [14] and quantum plasmonics [28–30] as well as the origin of above-threshold emission. For the latter, different interactions have been addressed [26, 31–33]. However, a complete picture and a systematic treatment are lacking.

Here, we develop a microscopic theory for plasmonic light emission in atomic-scale contacts based on the Keldysh nonequilibrium Green function (GF) formalism [34]. Our approach allows for a systematic calculation of the light emission to higher orders in the inter-

action between the tunnel current and localized surface-plasmon polaritons (LSPs) supported by the contact. LSPs are instrumental to light emission [29, 35, 36] and a direct probe of the quantum noise [6] due to their radiative nature and the enhanced electron-plasmon (e-pl) interaction which results from the strong local fields associated with them (see Fig. 1(a)). We here establish the link between the quantum noise and plasmonic light within the Keldysh GF formalism and furthermore discuss the relation to the AC conductance. Studying a generic contact model, we find that the experimentally observed above-threshold emission [6, 7] stems from higher-order contributions to the quantum noise associated with the plasmon-induced two-electron scattering process illustrated in Fig. 1(b).

We consider a single radiative LSP mode with frequency ω_{pl} (see Fig. 1(a)) represented by the quantized vector potential

$$\mathbf{A}(\mathbf{r}) = \boldsymbol{\xi}_{\text{pl}}(\mathbf{r}) \sqrt{\frac{\hbar}{2\Omega\epsilon_0\omega_{\text{pl}}}} (a^\dagger + a), \quad (2)$$

where Ω is a quantization volume and $\boldsymbol{\xi}_{\text{pl}}$ is a mode vector describing the spatial distribution of the field [37]. The

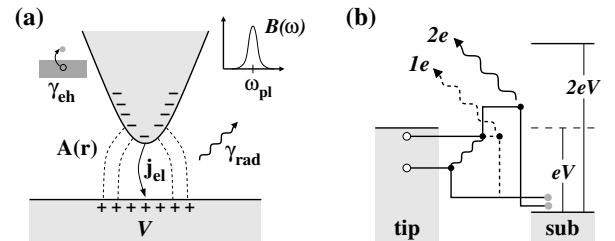


FIG. 1. (Color online) (a) Plasmonic STM contact. The inset illustrates the spectrum of the localized surface-plasmon polariton (LSP) supported by the contact. (b) Schematic illustration of the one and two-electron scattering processes responsible for the $1e$ (dashed lines; $\hbar\omega < eV$) and $2e$ (full lines; $eV < \hbar\omega < 2eV$) light emission.

interaction between the LSP and the tunnel current is given by the standard coupling term

$$H_{\text{el-pl}} = \int d\mathbf{r} \mathbf{j}_{\text{el}}(\mathbf{r}) \cdot \mathbf{A}(\mathbf{r}), \quad (3)$$

where $\mathbf{j}_{\text{el}} = \mathbf{j}_{\text{el}}^{\nabla} + \mathbf{j}_{\text{el}}^A$ is the electronic current density, and $\mathbf{j}_{\text{el}}^{\nabla}$ and \mathbf{j}_{el}^A the paramagnetic and diamagnetic components, respectively.

The excitation dynamics of the LSP and the emission is encoded in the LSP GF $D(\tau, \tau') = -i\langle T_c A(\tau) A(\tau') \rangle$ where $A = a + a^\dagger$ and T_c is the time-ordering operator on the Keldysh contour. The retarded and lesser components of the GF are given by their respective Dyson and Keldysh equations,

$$D^r(\omega) = d_0^r(\omega) + d_0^r(\omega) \Pi^r(\omega) D^r(\omega), \quad (4)$$

and

$$D^<(\omega) = D^r(\omega) \Pi^<(\omega) D^a(\omega), \quad (5)$$

where $d_0^r(\omega) = \frac{2\omega_{\text{pl}}}{(\omega + i0^+)^2 - \omega_{\text{pl}}^2}$ is the *bare* GF and $\Pi = \Pi_{\text{el}} + \Pi_{\text{rad}} + \Pi_{\text{eh}}$ is the *irreducible* self-energy which accounts for the interaction with the tunneling current (Π_{el}) as well as radiative decay (Π_{rad}) and decay into bulk electron-hole pair excitation (Π_{eh}). The latter two are modeled with phenomenological damping parameters $\gamma_{\text{rad/eh}}$ with self-energies $\Pi_{\text{rad/eh}}^r(\omega) = -i\gamma_{\text{rad/eh}} \text{sgn}(\omega)/2$ and $\Pi_{\text{rad/eh}}^{>/<}(\omega) = -i\gamma_{\text{rad/eh}} |n_B(\mp\omega)|$, where n_B is the Bose-Einstein distribution function, and give rise to a broadened LSP, $D_0^r(\omega) = \frac{2\omega_{\text{pl}}}{\omega^2 - \omega_{\text{pl}}^2 - i\omega_{\text{pl}}\gamma_0}$, with width $\gamma_0 = \gamma_{\text{rad}} + \gamma_{\text{eh}}$.

The excitation and broadening of the LSP due to the el-pl interaction (3) are governed by the el-pl self-energy, $\Pi_{\text{el}} = \Pi^{\nabla} + \Pi^A$. To lowest order in the interaction, the two contributions are given by [38]

$$\Pi^{\nabla}(\tau, \tau') = -i\langle T_c \delta j(\tau) \delta j(\tau') \rangle_0, \quad (6)$$

and

$$\Pi^A(\tau, \tau') = \delta(\tau - \tau') \langle \rho(\tau) \rangle_0, \quad (7)$$

respectively, where $\delta j = j - \langle j \rangle_0$,

$$j = \sqrt{\frac{\hbar}{2\Omega\epsilon_0\omega_{\text{pl}}}} \int d\mathbf{r} \boldsymbol{\xi}_{\text{pl}}(\mathbf{r}) \cdot \mathbf{j}_{\text{el}}^{\nabla}(\mathbf{r}) \quad (8)$$

is the projection of the current operator onto the LSP mode vector,

$$\rho = -\frac{e^2}{m_e} \frac{\hbar}{2\Omega\epsilon_0\omega_{\text{pl}}} \int d\mathbf{r} \boldsymbol{\xi}_{\text{pl}}(\mathbf{r}) \cdot \boldsymbol{\xi}_{\text{pl}}(\mathbf{r}) \Psi^\dagger(\mathbf{r}) \Psi(\mathbf{r}) \quad (9)$$

is the mode-weighted electron-density operator and $\langle \cdot \rangle_0$ is the expectation value in the absence of the el-pl interaction (3). The diamagnetic self-energy does not affect

the LSP dynamics as it only depends on the static charge density $\langle \rho \rangle_0$, and is here neglected.

From a perturbative expansion of the LSP GF in the paramagnetic interaction, we show that the *exact* paramagnetic self-energy is given by [39]

$$\Pi^{\nabla}(\tau, \tau') = -iS^{\text{irr}}(\tau, \tau'), \quad (10)$$

valid to all orders in the el-pl interaction. Here, S^{irr} is the *irreducible* part of the current-current correlation function $S(\tau, \tau') = \langle T_c \delta j(\tau) \delta j(\tau') \rangle$ [40] and the expectation value $\langle \cdot \rangle$ is with respect to the Hamiltonian that includes the el-pl interaction (3).

Focusing on the case where the el-pl coupling (8) is proportional to the current operator I , it follows from the important formal result (10) that the lesser self-energy $\Pi^{\nabla, <} = -iS_{\text{irr}}^<$ is given by the *irreducible* part of the quantum noise in Eq. (1). In addition, the retarded self-energy $\Pi^{\nabla, r} = -iS_{\text{irr}}^r$ is related to the response function $\mathcal{K}^r(t-t') = -i\Theta(t-t')\langle [I(t), I(t')] \rangle$, thus connecting the damping of the LSP to the dissipative real part of the AC conductance $\mathcal{G}(\omega) = i\mathcal{K}^r(\omega)/\omega$ of the contact. The quantities are connected via [41]

$$-2\omega \text{Re}\mathcal{G} = 2\text{Im}\mathcal{K}^r(\omega) = \mathcal{S}(\omega) - \mathcal{S}(-\omega), \quad (11)$$

which may be regarded as a *nonequilibrium* fluctuation-dissipation relation demonstrating the fundamental connection between quantum noise and AC conductance.

To connect the quantum noise to the light emission, we consider the radiative decay of the LSP into a reservoir of far-field modes, $H_{\text{far-field}} = \sum_{\lambda} \hbar\omega_{\lambda} a_{\lambda}^{\dagger} a_{\lambda}$, with the associated exchange rate per unit frequency given by

$$\Gamma_{\text{rad}}(\omega) = \Pi_{\text{rad}}^<(\omega) D^>(\omega) - \Pi_{\text{rad}}^>(\omega) D^<(\omega). \quad (12)$$

Here, the two terms account for absorption and emission, respectively, in agreement with Eq. (1) [41]. The emitted light is thus governed by $D^<(\omega) = -B(\omega) \frac{\Pi_{\text{el}}^<(\omega)}{2\text{Im}\Pi^r(\omega)} \stackrel{T=0}{=} -B(\omega) \frac{\Pi_{\text{el}}^<(\omega)}{2\text{Im}\Pi^r(\omega)}$, where $B = -2\text{Im}D^r$ is the LSP spectral function (see Fig. 1(a)), showing that it resembles the LSP spectrum and is driven by $\Pi_{\text{el}}^<$. With the above, we have established the link between plasmonic light emission and the quantum noise and AC conductance.

With the formal theory established, we go on to study the light emission and finite-frequency noise in a generic model for an atomic-scale STM contact consisting of a spin-degenerate electronic state/channel coupled to bulk lead reservoirs of the STM tip and substrate,

$$H = \varepsilon_0 \sum_{\sigma} d_{\sigma}^{\dagger} d_{\sigma} + \sum_{\alpha} H_{\alpha} + H_T + H_{\text{el-pl}} + \hbar\omega_{\text{pl}} a^{\dagger} a. \quad (13)$$

Here, $\varepsilon_0 = 0$ is the energy of the electronic level and $H_{\alpha} = \sum_k \varepsilon_{k,\alpha} c_{k\alpha}^{\dagger} c_{k\alpha}$, $\alpha = \{\text{tip, sub}\}$ is the Hamiltonian of the reservoirs with chemical potentials $\mu_{\text{tip/sub}} = \pm V/2$. The coupling to the reservoirs, $H_T =$

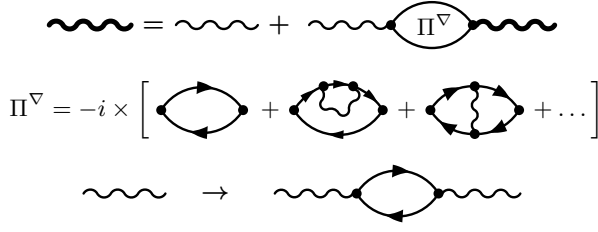


FIG. 2. (Color online) (top) Dyson equation for the LSP GF where Π^∇ denotes the paramagnetic el-pl self-energy. (center) Perturbation expansion of the self-energy showing the diagrams up to 4th order in the el-pl interaction. (bottom) The 6th order diagrams responsible for the $2e$ emission can be obtained by replacing the broadened LSP GF with its 2nd order correction (a plasmon excited by electron tunneling) in the 4th order diagrams. Feynman dictionary: •: el-pl interaction; solid lines: electronic contact GF $G_{ij}(\tau, \tau') = -i\langle T_c c_i(\tau) c_j^\dagger(\tau') \rangle_0$, $i, j = \text{tip, sub, d}$; thin wiggly lines: broadened LSP GF $D_0(\tau, \tau') = -i\langle T_c A(\tau) A(\tau') \rangle_0$.

$\sum_{\alpha, k} t_{k\alpha}^\alpha (c_{k\alpha}^\dagger d + \text{h.c.})$, leads to tunnel broadenings $\Gamma_\alpha = 2\pi\rho_\alpha |t_{k\alpha}|^2$ which define tunneling ($\Gamma_{\text{sub}} \ll \Gamma_{\text{tip}}$) and contact ($\Gamma_{\text{sub}} \sim \Gamma_{\text{tip}}$) regimes. In the two regimes, the electronic state can be associated with a localized state on the tip and a conduction channel of the contact, respectively. For $\Gamma = \Gamma_{\text{tip}} + \Gamma_{\text{sub}} \gg eV, k_B T$, the DC conductance is given by $\mathcal{G} = G_0 T$ where $G_0 = 2e^2/h$ and $T = 4\Gamma_{\text{tip}}\Gamma_{\text{sub}}/\Gamma^2$ is the transmission coefficient.

The el-pl interaction takes the form $H_{\text{el-pl}} = \sum_\alpha M_\alpha I_\alpha (a^\dagger + a)$, where $I_\alpha = i\sum_k (t_{k\alpha} c_{k\alpha}^\dagger d - \text{h.c.})$ is the paramagnetic current operator at reservoir α , $M_\alpha = \frac{e}{\hbar} \sqrt{\frac{\hbar}{2\Omega\epsilon_0\omega_{\text{pl}}}} \xi_\alpha l_\alpha$ is a dimensionless coupling constant, and $\xi_\alpha = \xi_{\text{pl}} \cdot \hat{\mathbf{e}}_\alpha$ and l_α is the projection of the mode vector onto the direction $\hat{\mathbf{e}}_\alpha$ of the current I_α and a characteristic length scale for the interaction, respectively. To describe the experimental light emission [6, 7], we take the el-pl coupling to be given by $|M_{\text{tip/sub}}| = M$ with $M_{\text{tip}} = -M_{\text{sub}}$, which implies that the LSP couples to the total current $I_{\text{tot}} = I_{\text{tip}} - I_{\text{sub}}$ through the contact [42]. The paramagnetic self-energy can now be written as a sum over lead-lead components, $\Pi^\nabla = \sum_{\alpha\beta} \Pi_{\alpha\beta}^\nabla$, where

$$\Pi_{\alpha\beta}^\nabla(\tau, \tau') = -iM_\alpha M_\beta S_{\alpha\beta}^{\text{irr}}(\tau, \tau'), \quad (14)$$

with $S_{\alpha\beta}(\tau, \tau') = \langle T_c \delta I_\alpha(\tau) \delta I_\beta(\tau') \rangle$ and $\delta I_\alpha = I_\alpha - \langle I_\alpha \rangle$. With the above-mentioned assumption for the coupling constant, we have $\Pi^\nabla(\tau, \tau') = -iM^2 S^{\text{irr}}(\tau, \tau')$ where $S(\tau, \tau') = \langle T_c \delta I_{\text{tot}}(\tau) \delta I_{\text{tot}}(\tau') \rangle$.

In the following, we proceed with a perturbative calculation of the *irreducible* el-pl self-energy illustrated in terms of Feynman diagrams in Fig. 2 (see Ref. [39] for details). We focus on the regime $\Gamma \gg \hbar\omega_{\text{pl}}, eV, k_B T$ and take $k_B T = 0$, corresponding to the experimentally relevant situation $k_B T \ll \hbar\omega_{\text{pl}}$ where the current is the only excitation source for the LSP.

Figure 3(a) shows the numerically calculated (*irre-*

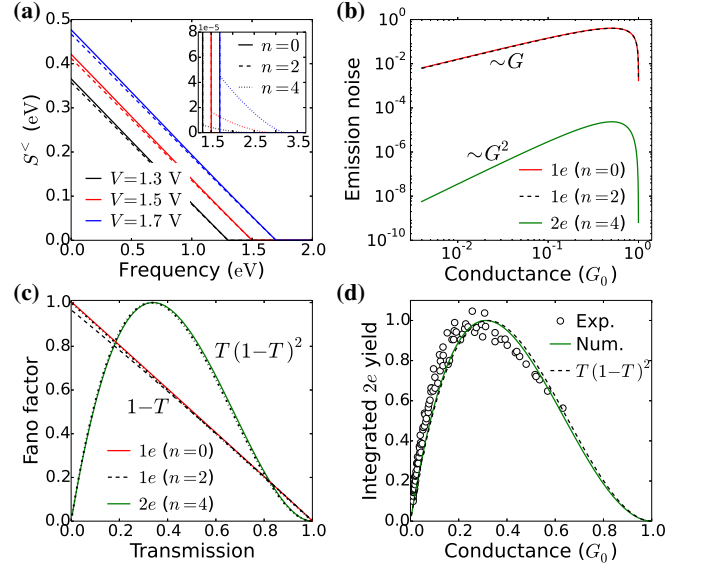


FIG. 3. (Color online) (a) Noise spectrum to different orders in the el-pl interaction ($n = 0$: solid, $n = 2$: dashed, and $n = 4$: dotted lines) for a contact with $T \sim 0.2$. The inset shows a zoom of the noise spectrum at $\omega \gtrsim eV$. (b) and (c) Integrated $1e$ and $2e$ emission noise and Fano factors at $V = 1.6$ V vs conductance and transmission, respectively. The dash-dotted lines in (c) show the indicated analytic functions. (d) Integrated $2e$ emission yield vs conductance at $V = 1.6$ V. The Fano factors and yield have been normalized to unity at their maximum value (the $1e$ Fano factors have been normalized with the $n = 0$ maximum). Parameters: $\omega_{\text{pl}} = 1.5$ eV, $\gamma_0 = 0.2$ eV, $M = 0.1$, $\Gamma_{\text{tip}} = 10$ eV.

ducible) emission noise to different orders in the el-pl interaction (the order of the corresponding self-energy is $n + 2$) for a contact with $T \sim 0.2$ and LSP parameters resembling the experiment [6]. The lowest-order ($n = 0$) *noninteracting* quantum noise (full lines in Fig. 3(a)) is given by the *bare* bubble diagram for which an analytic expression can be obtained for arbitrary contact parameters [39]. In the limit $\Gamma \gg eV, \hbar\omega, k_B T$, we find, in agreement with previous works [9, 43], that the *noninteracting* noise spectrum is given by [44]

$$S_0^<(\omega) \approx \frac{4 \times 2}{2\pi} [T(1-T) [H(\omega + eV) + H(\omega - eV)] + 2T^2 H(\omega)], \quad (15)$$

where $H(x) = xn_B(x)$. At $k_B T = 0$, the emission part simplifies to $S_0^<(\omega > 0) \sim T(1-T)\Theta(eV - \omega)(eV - \omega)$, and is hence suppressed at perfect transmission and cut off at $\omega = eV$, i.e. in this order only emission with $\omega < eV$ ($1e$) via the one-electron scattering process illustrated in Fig. 1(b) (dashed lines) is included.

The lowest-order corrections ($n = 2$)—a bubble with a “plasmon-dressed” contact GF and one with a vertex correction—give rise to a reduction of the emission noise

(dashed lines in Fig. 3(a) and are cut off at $\omega = eV$ like the *noninteracting* noise.

The above-threshold emission is contained in the 4th order ($n = 4$) quantum noise. At $k_B T = 0$, it originates from the coherent two-electron scattering process illustrated in Fig. 1(b), which corresponds to a plasmon-induced electron-electron (el-el) interaction. To identify the associated self-energy diagrams we employ the *optical theorem* stating that the imaginary part of a self-energy diagram is given by the sum of squared scattering amplitudes from possible “on-shell” cuts of the self-energy [45]. The relevant self-energy diagrams are therefore identified as the two $n = 2$ diagrams with the damped LSP GF replaced by its lowest-order correction (see bottom Fig. 2). The two diagrams give rise to the $\omega > eV$ component ($2e$) of the noise shown in the inset of Fig. 3(a) (dotted lines) which is cut off at $\omega = 2eV$. The cutoff stems from the above-mentioned scattering process where an initial emission process exciting the plasmon is followed by an absorption process generating a “hot electron” which can emit at above-threshold energies $eV < \omega < 2eV$. At finite temperature, “hot electrons” can also be generated from thermally excited plasmons. However, at $k_B T \ll \hbar\omega_{\text{pl}}$ this process is negligible.

To further analyze the quantum noise, we show in Figure 3(b) the integrated $1e$ ($0 < \omega < eV$) and $2e$ ($eV < \omega < 2eV$) components [6, 7] of the emission noise at $V = 1.6$ V as a function of the conductance. In the tunneling regime, $\mathcal{G} \ll G_0$, the noise components are found to scale with the conductance as $S_{1e}^< \sim \mathcal{G}$ and $S_{2e}^< \sim \mathcal{G}^2$, respectively, emphasizing that they involve one and two-electron scattering processes. Moreover, at perfect transmission, $\mathcal{G} \sim G_0$, both the $1e$ and $2e$ noise are suppressed. For the $1e$ noise, the $n = 2$ corrections do not change this qualitatively. We emphasize that the suppression of emission noise at $T = 1$ only holds in the considered large- Γ limit [39].

The fact that the $2e$ noise shows a \mathcal{G}^2 dependence in the tunneling regime and is suppressed at contact, suggests that it scales as the square of the prefactor in the *noninteracting* noise, i.e. $S_{2e}^< \sim T^2(1 - T)^2$. To test this hypothesis, we inspect the finite-frequency Fano factor $F(\omega) = \mathcal{S}(\omega)/eI$ which should then scale with the transmission coefficient as

$$F_{1e} \sim 1 - T \quad \text{and} \quad F_{2e} \sim T(1 - T)^2, \quad (16)$$

with the maximum of F_{2e} occurring at $T = 1/3$. The integrated Fano factors shown in Fig. 3(c) are in excellent agreement with our expectations, confirming the anticipated scaling of the $2e$ emission noise. The ratio of the $1e$ and $2e$ emission noise thus scales with the coupling constant and transmission coefficient as $S_{2e}^</math>$

Next, we discuss the emission spectrum shown in Fig. 4 as a function of bias voltage and conductance. As expected, the emission which resembles the LSP spectrum

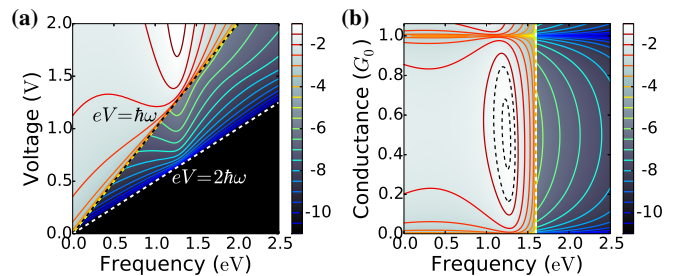


FIG. 4. (Color online) (a) Emission spectrum vs applied voltage for a contact with $T \sim 0.2$. (b) Emission spectrum vs transmission coefficient at $V = 1.6$ V. The plots show the emission rate $\Gamma_{\text{rad}}(\omega) \propto -\text{Im}D^<(\omega)$ in units of γ_{rad} on a logarithmic scale. Parameters: $\omega_{\text{pl}} = 1.5$ eV, $\gamma_0 = 0.2$ eV, $M = 0.1$, $\Gamma_{\text{tip}} = 10$ eV.

has a dominant $1e$ component which is driven by the *noninteracting* quantum noise, and a weaker $2e$ component driven by the higher-order quantum noise. Due to the predicted T dependence of the quantum noise, both the $1e$ and $2e$ emission peak at $\mathcal{G} \sim 0.5 G_0$ and are strongly reduced at $\mathcal{G} \sim G_0$. This counter intuitive behavior at perfect transmission where the current is maximized and one naively would expect the same for the emission, is a unique fingerprint of the quantum noise origin.

The tunneling-induced damping of the LSP associated with the dissipative part of the AC conductance gives rise to an additional spectral broadening $\gamma_{\text{el}} = -2\text{Im}\Pi^{\nabla,r}$. In the large Γ -limit and to lowest order in the el-pl interaction, $\text{Re}\mathcal{G}(\omega) = G_0 T$ and $\gamma_{\text{el}} = 8\omega/\pi M^2 T$. Contrary to the emission noise, it does not vanish at $T = 1$ and is independent of the bias voltage. Due to the nondissipative part of the AC conductance (real part of the self-energy) the LSP resonance redshifts (~ 0.1 eV) with increasing conductance in Fig. 4(b). Similar spectral features have been observed in subnanometer plasmonic contacts [28, 46], though the importance of tunneling versus other mechanisms is unclear [47–51]. Our findings indicate that electron tunneling plays a nonnegligible role in the quantum regime.

Finally, in Fig. 3(d) we show the calculated $2e$ emission yield, defined as emission per current, as a function of conductance together with the experimental $2e$ photon yield from Ref. [6]. Compared to the Fano factor in Fig. 3(c), the above-mentioned spectral changes result in a slight left shift of the curve for the yield. The agreement with the experimental $2e$ yield is very good, indicating that we have identified the mechanism responsible for $2e$ emission. At $\mathcal{G} \sim G_0$, however, the experimental yields do not show complete suppression (see Ref. [6]). This discrepancy can be due to experimental factors such as: (i) imperfect or additional transmission channels [6], and/or (ii) changes in the LSP mode and el-pl coupling as the tip-substrate distance is reduced [52].

To summarize, we have presented a framework based

on the Keldysh GF formalism for the description of light emission from plasmonic contacts and established the connection between the quantum noise and AC conductance of the contact and the light emission. Studying a generic contact model, we have identified a plasmon-induced el-el interaction associated with the higher-order quantum noise as the mechanisms behind the experimentally observed above-threshold emission [6, 7]. Our approach, which can be generalized to more complex situations, paves the way for a better understanding of the effect of interactions on light emission from atomic-scale and molecular contacts.

We would like to thank W. Belzig, T. Novotný, M. Galperin, N. A. Mortensen, J. Paaske and M. Brandbyge for fruitful discussions, R. Berndt for providing us with the original data from Ref. 6 and M. H. Fischer for comments on the manuscript. This research was supported by the Israel Science Foundation, the Israel-US Binational Science Foundation (grant No. 2011509), and the European Science Council (FP7/ERC grant No. 226628). AN thanks the Physics Department at FUB and SFB 658 for hospitality during the time this work was completed. KK acknowledges support from the Villum Kann Rasmussen and Carlsberg Foundations.

* cosby@fys.ku.dk

- [1] N. Agraït, A. L. Yeyati, and J. M. van Ruitenbeek, *Physics Reports* **377**, 81 (2003).
- [2] L. Olesen, E. Laegsgaard, I. Stensgaard, F. Besenbacher, J. Schiøtz, P. Stoltze, K. W. Jacobsen, and J. K. Nørskov, *Phys. Rev. Lett.* **72**, 2251 (1994).
- [3] H. E. van den Brom and J. M. van Ruitenbeek, *Phys. Rev. Lett.* **82**, 1526 (1999).
- [4] N. Agraït, C. Untiedt, G. Rubio-Bollinger, and S. Vieira, *Phys. Rev. Lett.* **88**, 216803 (2002).
- [5] M. Kumar, R. Avriller, A. L. Yeyati, and J. M. van Ruitenbeek, *Phys. Rev. Lett.* **108**, 146602 (2012).
- [6] N. L. Schneider, G. Schull, and R. Berndt, *Phys. Rev. Lett.* **105**, 026601 (2010).
- [7] G. Schull, N. Néel, P. Johansson, and R. Berndt, *Phys. Rev. Lett.* **102**, 057401 (2009).
- [8] G. B. Lesovik and R. Loosen, *Pis'ma Zh. Eksp. Teor. Fiz.* **65**, 280 (1997), [*JETP Lett.* 65, 295 (1997)].
- [9] R. Aguado and L. P. Kouwenhoven, *Phys. Rev. Lett.* **84**, 1986 (2000).
- [10] U. Gavish, Y. Levinson, and Y. Imry, *Phys. Rev. B* **62**, 10637 (2000).
- [11] C. W. J. Beenakker and H. Schomerus, *Phys. Rev. Lett.* **86**, 700 (2001).
- [12] Z. C. Dong, X. L. Zhang, H. Y. Gao, Y. Luo, C. Zhang, L. G. Chen, R. Zhang, X. Tao, Y. Zhang, J. L. Yang, et al., *Nature Phot.* **4**, 50 (2010).
- [13] N. L. Schneider, J. T. Lü, M. Brandbyge, and R. Berndt, *Phys. Rev. Lett.* **109**, 186601 (2012).
- [14] M. Galperin and A. Nitzan, *Phys. Chem. Chem. Phys.* **14**, 9421 (2012).
- [15] J.-T. Lü, R. B. Christensen, and M. Brandbyge, *Phys. Rev. B* **88**, 045413 (2013).
- [16] G. Reecht, F. Scheurer, V. Speisser, Y. J. Dappe, F. Mathevet, and G. Schull, *Phys. Rev. Lett.* **112**, 047403 (2014).
- [17] E. Zakka-Bajjani, J. Ségala, F. Portier, P. Roche, D. C. Glattli, A. Cavanna, and Y. Jin, *Phys. Rev. Lett.* **99**, 236803 (2007).
- [18] E. A. Rothstein, O. Entin-Wohlman, and A. Aharony, *Phys. Rev. B* **79**, 075307 (2009).
- [19] A. A. Clerk, M. H. Devoret, S. M. Girvin, F. Marquardt, and R. J. Schoelkopf, *Rev. Mod. Phys.* **82**, 1155 (2010).
- [20] J. Basset, H. Bouchiat, and R. Deblock, *Phys. Rev. Lett.* **105**, 166801 (2010).
- [21] A. V. Lebedev, G. B. Lesovik, and G. Blatter, *Phys. Rev. B* **81**, 155421 (2010).
- [22] M. Hofheinz, F. Portier, Q. Baudouin, P. Joyez, D. Vion, P. Bertet, P. Roche, and D. Esteve, *prl* **106**, 217005 (2011).
- [23] C. P. Orth, D. F. Urban, and A. Komnik, *Phys. Rev. B* **86**, 125324 (2012).
- [24] R. Zamoum, A. Crépieux, and I. Safi, *Phys. Rev. B* **85**, 125421 (2012).
- [25] C. Altimiras, O. Parlavecchio, P. Joyez, D. Vion, P. Roche, D. Esteve, and F. Portier, *Phys. Rev. Lett.* **112**, 236803 (2014).
- [26] F. Xu, C. Holmqvist, and W. Belzig, *Phys. Rev. Lett.* **113**, 066801 (2014).
- [27] J.-C. Forgues, C. Lupien, and B. Reulet, *Phys. Rev. Lett.* **113**, 043602 (2014).
- [28] K. J. Savage, M. M. Hawkeye, R. Esteban, A. G. Borisov, J. Aizpurua, and J. J. Baumberg, *Nature* **491**, 574 (2012).
- [29] P. Bharadwaj, A. Bouhelier, and L. Novotny, *Phys. Rev. Lett.* **106**, 226802 (2011).
- [30] M. S. Tame, K. R. McEnery, Ş. K. Özdemir, J. Lee, S. A. Maier, and M. S. Kim, *Nature Phys.* **9**, 329 (2013).
- [31] G. Hoffmann, R. Berndt, and P. Johansson, *Phys. Rev. Lett.* **90**, 046803 (2003).
- [32] J. Tobiska, J. Danon, I. Snyman, and Y. V. Nazarov, *Phys. Rev. Lett.* **96**, 096801 (2006).
- [33] N. L. Schneider, P. Johansson, and R. Berndt, *Phys. Rev. B* **87**, 045409 (2013).
- [34] H. Haug and A.-P. Jauho, *Quantum Kinetics in Transport and Optics of Semiconductors* (Springer, Berlin, 1998).
- [35] P. Johansson, R. Monreal, and P. Apell, *Phys. Rev. B* **42**, 9210 (1990).
- [36] R. Berndt, J. K. Gimzewski, and P. Johansson, *Phys. Rev. Lett.* **67**, 3796 (1991).
- [37] P. Johansson, *Phys. Rev. B* **58**, 10823 (1998).
- [38] G. D. Mahan, *Many-particle Physics* (Springer, 2010), 3rd ed.
- [39] K. Kaasbjerg and A. Nitzan, in preparation.
- [40] We use the symbols S and \mathcal{S} for the correlation function in units of eV and $\frac{e^2}{s}$, respectively. The replacement $\frac{1}{2\pi} \leftrightarrow \frac{e^2}{h}$ switches between the two.
- [41] This follows from the relations $S^r - S^a = S^> - S^<$, $S^>(\omega) = S^<(-\omega)$ and $D^>(\omega) = D^<(-\omega)$.
- [42] As opposed to charge fluctuations of the contact, $\Delta I = I_{\text{tip}} + I_{\text{sub}}$, which would be the case if $M_{\text{tip}} = M_{\text{sub}}$.
- [43] Y. M. Blanter and M. Büttiker, *Phys. Rep.* **336**, 1 (2000).
- [44] The factor of 4 in Eq. (15) stems from the fact that the total noise, $S^< = \sum_{\alpha\beta} S_{\alpha\beta}^<$, is considered.

- [45] A. Zee, *Quantum Field Theory in a Nutshell* (Princeton University Press, Princeton, 2010), 2nd ed.
- [46] J. A. Scholl, A. García-Etxarri, A. L. Koh, and J. A. Dionne, *Nano. Lett.* **13**, 564 (2013).
- [47] P. Song, P. Nordlander, and S. Gao, *J. Chem. Phys.* **134**, 074701 (2011).
- [48] R. Esteban, A. G. Borisov, P. Nordlander, and J. Aizpurua, *Nature Comm.* **3**, 825 (2012).
- [49] N. A. Mortensen, S. Raza, M. Wubs, T. Søndergaard, and S. I. Bozhevolnyi, *Nature Comm.* **5**, 3809 (2014).
- [50] T. V. Teperik, P. Nordlander, J. Aizpurua, and A. G. Borisov, *Phys. Rev. Lett.* **110**, 263901 (2013).
- [51] T. V. Teperik, P. Nordlander, J. Aizpurua, and A. G. Borisov, *Optics Express* **21**, 27306 (2013).
- [52] J. Aizpurua, G. Hoffmann, S. P. Apell, and R. Berndt, *Phys. Rev. Lett.* **89**, 156803 (2002).